NASA/CR- —96— 207497

final NAGW-3981

March 2, 1998

Validation of the Version 1 NOAA/NASA Pathfinder Sea Surface Temperature Data Set

IN-48-CR
076551

Elizabeth A. Smith
Research Assistant Professor
Center for Coastal Physical Oceanography
Department of Ocean, Earth and Atmospheric Sciences
Old Dominion University

1. Background

A high-resolution, global satellite-derived sea surface temperature (SST) data set called Pathfinder, from the Advanced Very High Resolution Radiometer (AVHRR) aboard the NOAA Polar Orbiters, is available from the Jet Propulsion Laboratory Physical Oceanography Distributed Active Archive Center (JPL PO.DAAC). Suitable for research as well as education, the Pathfinder SST data set is a result of a collaboration between the National Oceanographic and Atmospheric Administration (NOAA), the National Aeronautics and Space Administration (NASA) and investigators at several universities. NOAA and NASA are the sponsors of the Pathfinder Program, which takes advantage of currently archived Earth science data from satellites. Where necessary, satellite sensors have been intercalibrated, algorithms improved and processing procedures revised, in order to produce long time-series, global measurements of ocean, land and atmospheric properties necessary for climate research. Many Pathfinder data sets are available to researchers now, nearly a decade before the first launch of NASA's Earth Observing System (EOS). The lessons learned from the Pathfinder programs will facilitate the processing and management of terabytes of data from EOS. The Oceans component of Pathfinder has undertaken to reprocess all Global Area Coverage (GAC) data acquired by the 5-channel AVHRRs since 1981. The resultant data products are consistent and stably calibrated [*Rao,* 1993a, *Rao,* 1993b, *Brown et al.*, 1993)], Earth-gridded SST fields at a variety of spatial and temporal resolutions.

2. Introduction

This technical report describes a statistical analysis of the Version 1 Pathfinder SST data set, as compared with global moored and drifting buoy data from the AVHRR Pathfinder Oceans Matchup Database 1985-1993 (Version 18) which was produced by the Remote Sensing Group at the University of Miami, Rosenstiel School of Marine and Atmospheric Sciences (Podesta et al, 1995). Section 3 contains a description of the methods and algorithms used to derive SST from AVHRR measurements. A discussion of AVHRR Pathfinder Version 1 algorithms will be covered in this section. Geophysical factors effecting the accuracy of satellite-derived estimates of SST are discussed briefly in Section 4. Section 5 contains a discussion of the validation analyses and results.

Since 1993, the PO.DAAC at JPL has been distributing daily, global AVHRR-derived SST fields from the NOAA/NASA AVHRR Pathfinder Program. Data for the period from January 1987 - May 1991 have been distributed to hundreds of users. These data were processed using approved Pathfinder AVHRR Version 1 algorithms and coefficients (Vazquez, 1995 - User's Guide). In June of 1997, a new Pathfinder SST algorithm was approved by the Science Working Group, known as Version 4 (Evans et al, 1996, Vazquez, 1996). The JPL PO.DAAC is in the process of reprocessing all of the AVHRR data using the Version 4 algorithms. For a description of data availability and a discussion of the Version 4 algorithms, see http://podaac.jpl.nasa.gov/sst/, which is the JPL PO.DAAC WWW homepage for the Pathfinder data.

3. Description of Version 1 Algorithms and Coefficients for the Pathfinder SST Project

The AVHRR Level-1B sensor counts in the visible channels (1 and 2) are first converted to Rayleigh-corrected radiances and then to optical depth for use in removing the effects of the atmosphere and viewing and illumination geometry. Channels 3, 4 and 5 are transformed to units of "brightness temperature", using the Planck black body function and a newly-determined correction for sensor calibration non-linearity in the longer-wavelength channels (Brown et al., 1993). Version 1 (V1) of the Pathfinder SST algorithm is essentially the nonlinear SST (NLSST) (Walton, 1988), with a modification for sensor calibration drift with time. The V1 algorithm is also conditioned in three different atmospheric regimes based on the difference between Channel 4 and Channel 5 (Ch. 4 minus Ch. 5), and unique regression coefficients are applied in each regime. The form of the V1 algorithm is:

$$SST = a + b*T4 + c*(T4-T5)*Tsurf + d*(\sec(q)-1)*(T4-T5) + e*lifetime \quad (1)$$

where q is the zenith angle of the instrument, and T4 and T5 are the brightness temperatures from AVHRR channels 4 and 5, respectively, as determined using the procedure outlined in NOAA Technical Report NESDIS 69. Tsurf is an a-priori estimate of the SST. It is derived from the 1-degree optimum interpolated SST analysis produced by Dr. Richard Reynolds of NOAA/NESDIS (Reynolds and Smith, 1994), which has been interpolated to the nominal 9km grid. The spatial interpolation used is a bilinear interpolation of the 4 closest neighboring points surrounding the nominal 9km grid point. The empirical coefficients a, b, c, d, and e are determined through a multiple-regression of AVHRR radiances with a database of *in-situ* temperatures, measured using moored and drifting buoys (Podesta, 1995). These coefficients are calculated for one year at a time, in three atmospheric regimes as defined by the difference between T4 and T5. To be considered a match, the pixel location of the satellite-derived measurement and *in-situ* measurement must fall within 0.1 degree spatially, and 30 minutes of one another. Recently, the AVHRR thermal vacuum test data have been examined in detail (Brown et. al., 1993) in order to quantify the temporal drift in the calibration of the AVHRR channels. Through this work, the nonlinear SST algorithm first developed by Walton (1988) was modified with a time-dependent term, called lifetime in (1).

Table 1 shows the coefficients used in deriving the sea surface temperatures for the Version 1 Pathfinder SST data set for 1987-1988.

Table 1
NOAA-9: for years 1987 and 1988, not valid before 1987

a	b	c	d	e	channel 4-5 range
1.600	**0.930**	**0.149**	**0.085**	**-0.029**	**< 0.7**
2.202	**0.953**	**0.089**	**0.673**	**-0.086**	**0.7< 1.8**
4.470	**0.868**	**0.090**	**0.439**	**-0.176**	**=1.8**

NOAA-11: valid from launch Nov. , 1988 until May , 1991; not valid afterwards.

a	b	c	d	e	channel 4-5 range
1.011	**0.934**	**0.120**	**1.118**	**0.026**	**< 0.7**
1.336	**0.945**	**0.087**	**0.984**	**0.003**	**0.7 < 1.8**
3.250	**0.869**	**0.078**	**0.805**	**0.009**	**= 1.8**

4. Summary of Known Errors

Much work has been done to date to identify and quantify the variability of AVHRR-derived SST measurements. At any given location we know the SST variability (the departure from the climatological mean) may range from a few tenths of a degree to as much as 5-7 degrees (under El Nino conditions, for instance). SST algorithms must be robust in order to work under a this range of environmental conditions. Described below are some of the better understood sources of error in the retrieval of satellite SSTs.

a. Differences between the skin and the bulk temperature

Multichannel algorithms for estimating SST from the AVHRR, such as the MCSST, NLSST and Pathfinder NLSST, do not take into account the difference between the ocean's skin temperature (what the AVHRR actually sees and measures) and underlying mixed layer SST which is referred to as the "bulk" temperature. The "bulk" temperature is the quantity measured by most buoys. The uppermost millimeter of the ocean, or skin, can be as much as 0.7 °C cooler than the water just below (*Ewing and McAlister*, 1960) due to evaporative or radiative cooling. Conditioning the satellite-derived SST estimates using buoys, as is done in the Pathfinder SST algorithms and their predecessors, results in a measurement which more closely resembles a "bulk" SST estimate, not a skin estimate (*Schluessel et al.*, 1990).

b. *Problems with buoys*

In situ measurement of SST is a complicated task, and hence, there is the potential that errors exist both in archived *in situ* SSTs and in satellite SST derivation procedures using *in situ* SST. Heating or cooling of the sea surface occurs as a result of air-sea fluxes, horizontal and vertical heat advection, and mixing. It is the nature of the air-sea fluxes of heat that complicates the measurement of SST in the ocean.

c. Cloud contamination

A significant limitation of satellite-derived SST measurements is the inability to make AVHRR SST measurements in the presence of clouds. Most of the time, this limitation is overcome by performing temporal averaging or compositing over weeks and months, and over large spatial scales. For some applications, this is not always feasible. In regions of persistent high cloudiness, even monthly composites exhibit data voids. Cloud detection techniques are generally applied globally and in an automated fashion especially when global data sets are produced in an operational environment. The drawback to such techniques is that there will inevitably be mistakes because of the strong regional and temporal variability in cloud formation and movement. Cloudy pixels will be determined to be valid SSTs and perfectly good SSTs will be discarded as clouds. For the Pathfinder SST data sets, these cloud detection techniques are being carefully scrutinized.

d. Aerosols and water vapor

SST estimates in regions of high humidity (such as the western equatorial Pacific Ocean) require large atmospheric corrections. Likewise, volcanic aerosols, such as were detected in the stratosphere in abundance following the eruptions of El Chichon in 1982 and again in 1991 after Mt. El Pinatubo erupted in the Philippines, have been found to bias the SST retrievals anomalously low.

5. Validation Approach

The objective of this grant was to provide validation statistics for the Version 1 Pathfinder SST global data set for 1987-1990.

a. Description of Version 1 Pathfinder SST Data

The data used in this validation study are daily gridded fields with a nominal spatial resolution of 9 kilometers. Ascending and descending passes are separated during production and hence considered separately during analysis. For this study, to reduce the data volume, only the de-clouded data (a.k.a., the best SST) are considered. The SST algorithms are as described in Section 3 above.

b. Description of the AVHRR Pathfinder Oceans Matchup Database(1987-1990) Version 18.

The *in situ* SST data set against which the satellite-derived Pathfinder SST observations are compared is the AVHRR Pathfinder Oceans Matchup Database(1987-1990) Version 18. This is a multi-satellite, multi-year database of AVHRR and high-quality, in situ SST matchups. The in situ SST data come from two sources, moored and drifting buoys, from a variety of agencies and programs worldwide.

6. Results

Figure 1 shows the global distribution of the moored and drifting buoy data in the Version 1 Matchup data base for the period 1987-1990. Coverage is excellent in some regions (eastern Equatorial Pacific Ocean) and poor in others (tropical Atlantic and Indian Oceans). There are an order of magnitude more moored buoy observations of SST in the Northern Hemisphere than the Southern Hemisphere. On the other hand, there are more drifter data in the Southern Hemisphere than the Northern Hemisphere. Figure 2 shows the distribution of moored and drifting buoy data for 1987, a representative year.

A residual is defined as buoy SST minus the satellite-derived Pathfinder SST. Residuals and Root Mean Square (RMS) errors are computed for every matchup pair for each day from January 1987 thru April 1991 and shown as a time series in Figure 3. The average residual (also called bias) is 0.08oC and the average RMS error is 0.82oC. A small positive bias of 0.08oC indicates that, globally, the Pathfinder SST satellite-derived data are slightly cooler than the buoy SST data. Cloud contamination in the Pathfinder SST fields would explain this low bias as would the presence of water vapor in the atmosphere.

Separating the matchup pairs of buoy and Pathfinder SST based upon latitude and then computing the statistics helps elucidate the mechanisms contributing to the computed residuals. Figures 4 and 5 show time series plots of residuals and RMS errors, respectively, for three bands of latitude; 20N to 50N, 20N to 20S and 20S to 50S. Average residuals in the subtropical northern latitudes (top panel of Figure 4) are negative, meaning the Pathfinder SST data are warmer than the buoy SSTs. The RMS errors for the subtropical northern latitudes (top panel of Figure 5) show a seasonal cycle with largest RMS errors in the summer months. Large RMS errors correspond to periods of negative residuals for latitudes north of 20N. Negative residuals in the summer months in the northern hemisphere subtropics are probably a result of intense solar heating of the ocean's skin in the subtropical gyres, in the presence of low winds. Since the AVHRR instrument measures of this skin temperature, it is not surprising that the Pathfinder SST data are biased warm north of 20N.

The highest average residuals are found in the tropics (middle plot of Figure 4), where atmospheric water vapor is high. Variability in the tropics is lower than either the subtropical northern or southern latitudes. Water vapor in the atmosphere is the most likely contributing mechanism to the observed warm bias in the tropics.

In addition to computing residuals and RMS errors globally, they were computed for six oceanic regions, for each year; Eastern Tropical Pacific Ocean, East Coast of North America/Gulf of Mexico, North Atlantic Ocean, Southern Indian & Atlantic Oceans, West Coast of North America/Eastern Pacific and the Indian Ocean. Table 2-Table 5 show these results. Negative residuals between the Pathfinder SST and the in situ data are seen for each year in East Coast of North America/Gulf of Mexico region. As was discussed in the previous paragraph, a warm bias such as this is probably the result of the satellite measuring the warmer skin layer of the ocean, and the buoy measuring the bulk SST. The smallest residuals are computed for observations in the West Coast of North America/Eastern Pacific while the largest residuals are found in the Indian Ocean, where there is a strong seasonal cycle. More interpretation of these regional results is currently underway with the introduction of a satellite- derived water vapor data set from the Special Sensor Microwave Imager in order to elucidate the role of water vapor in biasing satellite SST measurements.

REFERENCES

Brown J. W., O. B. Brown, and R. H. Evans, 1993. Calibration of AVHRR infrared channels: a new approach to non-linear correction, Journal of Geophysical Research, 98 (NC10), 18257-18268.

Evans, R. H., and G. Podesta, 1996. Second report to the sea surface temperature science working group, University of Miami, RSMAS, February, 1996.

Ewing G., and E. D. McAlister, 1960. On the thermal boundary layer of the ocean, Science, 131, 1374-1376.

McClain E. P., W. G. Pichel, and C. C. Walton, 1985. Comparative performance of AVHRR based multichannel sea surface temperatures, Journal of Geophysical Research 90, 11587-11601.

Podesta, G. P., S. Shenoi, J. W. Brown, and R. H. Evans, 1995. AVHRR Pathfinder Oceans Matchup Database 1985-1993 (Version 18), Report from the University of Miami, Rosenstiel School of Marine and Atmospheric Science, June 1995, 33pp.

Rao, C. R. N., 1993. Degradation of the visible and near-infrared channels of the Advanced Very High Resolution Radiometer on the NOAA-9 spacecraft: Assessment and recommendations for corrections, NOAA Technical Report 68, January 1993, 42pp.

Rao, C. R. N., 1993. Nonlinearity corrections for the thermal infrared channels of the Advanced Very High Resolution Radiometer: Assessment and recommendations, NOAA Technical Report 69, February 1993, 43pp.

Reynolds, R. W. and T. M. Smith, 1994. Improved global sea surface temperature analyses using optimum interpolation. Journal of Climate, 7, 929-948.

Schluessel, P., W.J. Emery, H. Grassl, and T. Mammen, 1990. On the bulk-skin temperature difference and its impact on satellite-remote sensing of sea surface temperature, Journal of Geophysical Research, 95(C8), 13341-13356.

Vazquez, J. and A. Tran, R. Sumagaysay, E. A. Smith and M. Hamilton, 1995. NOAA/NASA AVHRR Oceans Pathfinder Sea Surface Temperature Data Set User's Guide Version 1.2, JPL Technical Report, 53pp.

Walton, C. C., 1988. Nonlinear multichannel algorithms for estimating sea surface temperature with AVHRR satellite data, Journal of Applied Meteorology, 27, 115-124.

Walton, C. C., E. P. McClain, and J. F. Sapper, 1990. Recent changes in satellite- based multichannel sea surface temperature algorithms, Rep. MTS 90, Mar. Technol. Soc., Washington, D.C., September 1990.

Figure 1

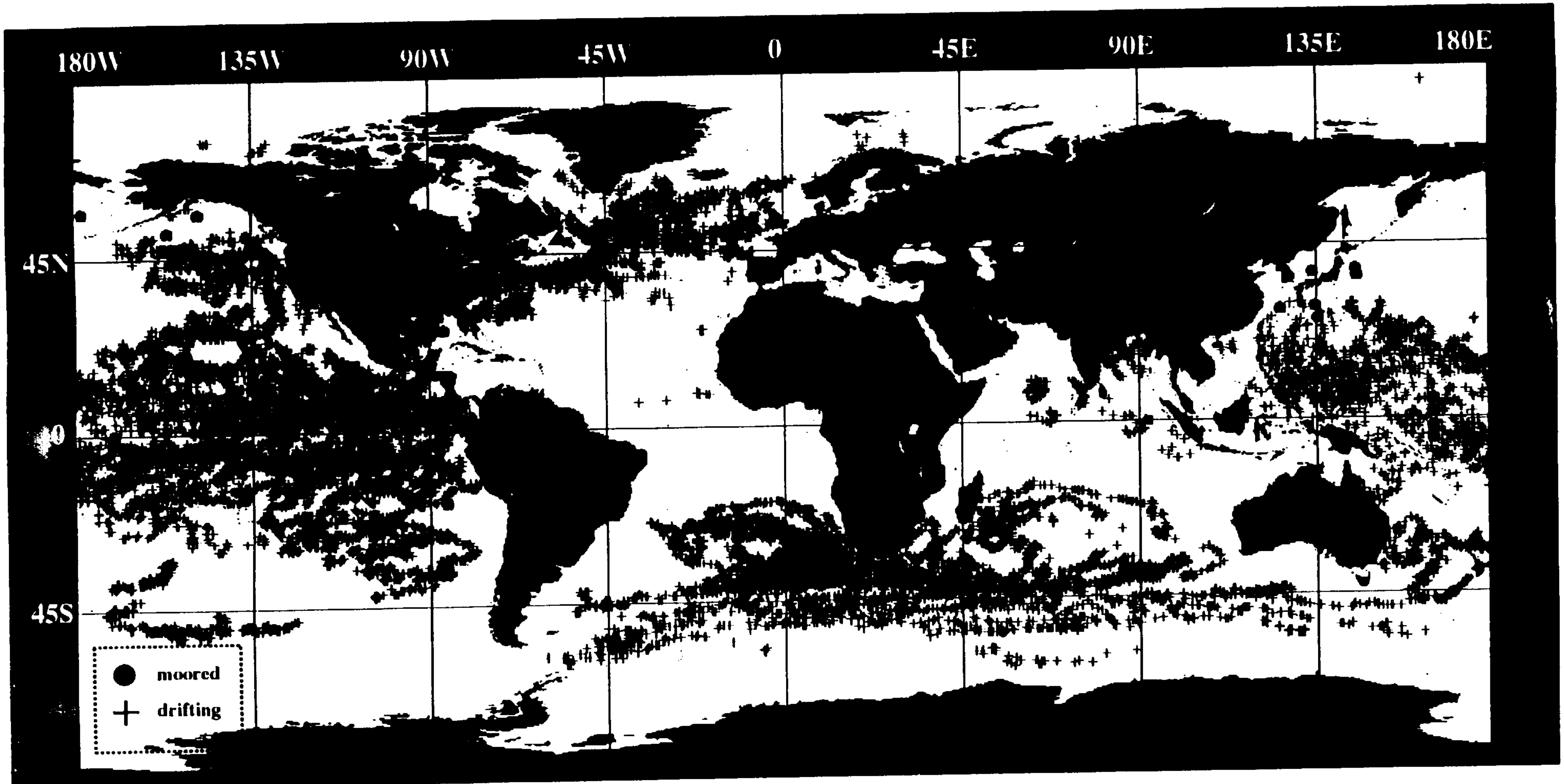

Geographic distribution of buoy/satellite matchups for NOAA–9 and NOAA–11 (1987 – 1990)

1987 - ZONAL DISTRIBUTION of MATCHUPS

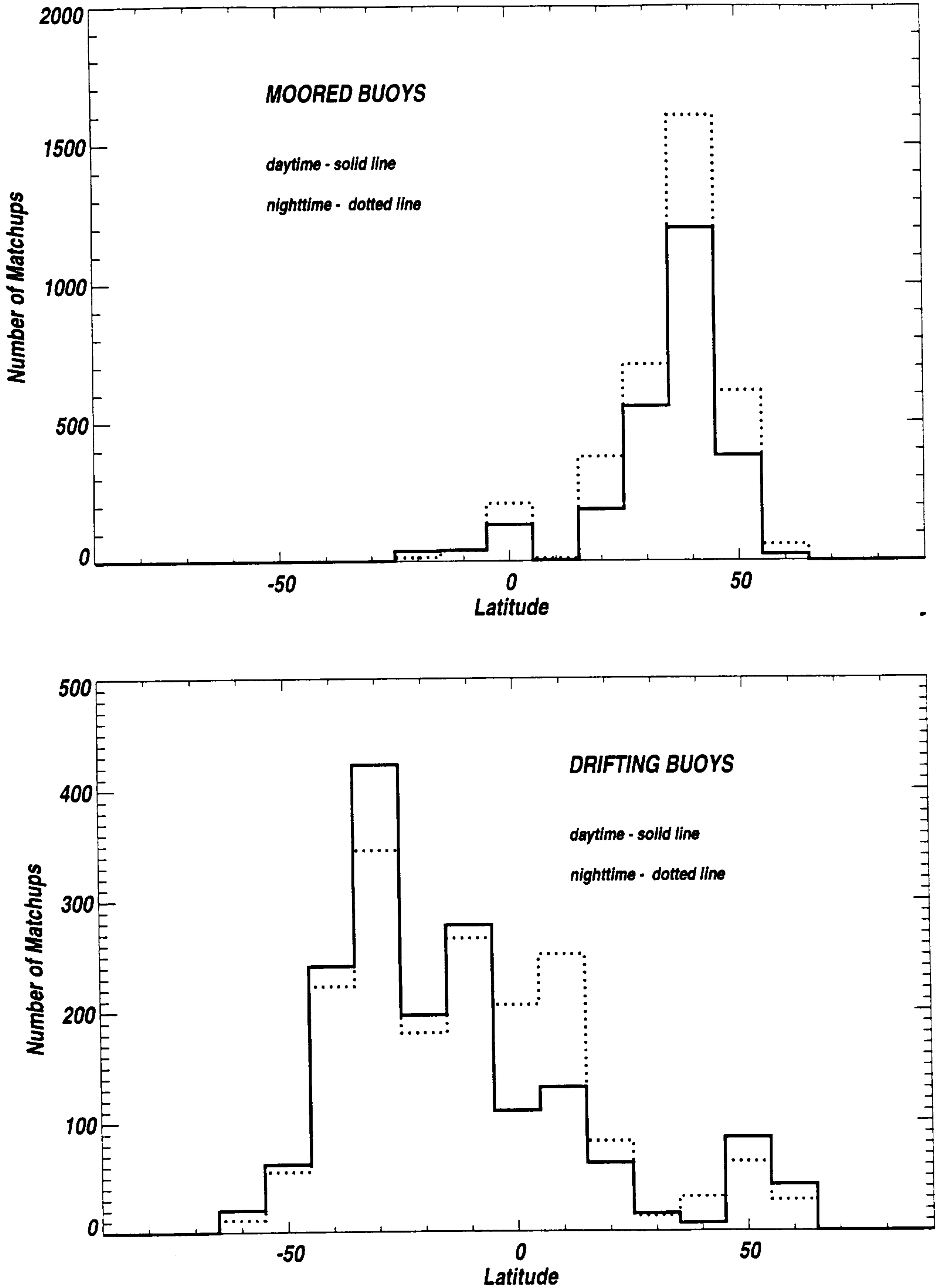

Figure 2

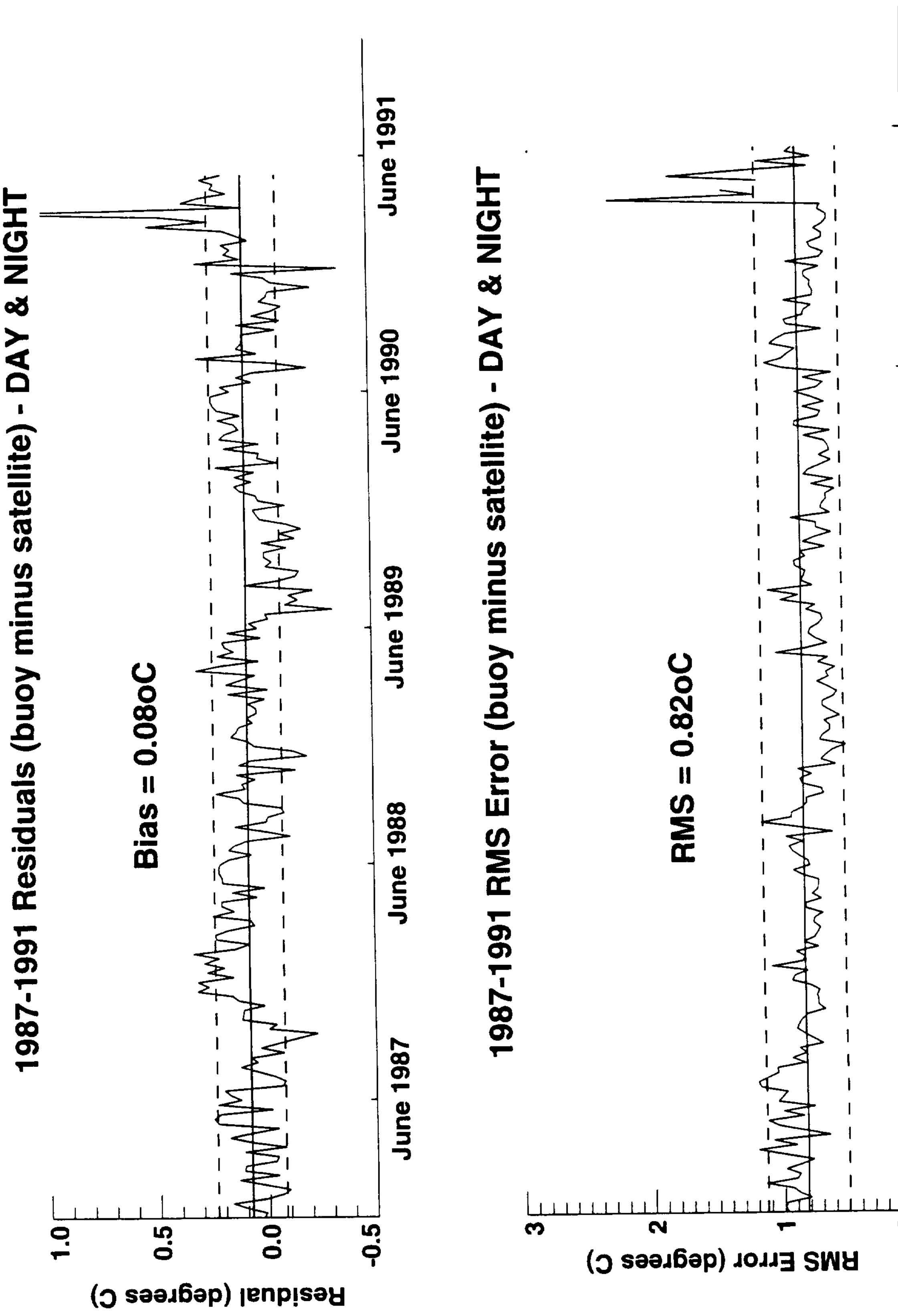
1987-1991 Residuals (buoy minus satellite) - DAY & NIGHT
Bias = 0.08oC
Residual (degrees C)
1.0
0.5
0.0
-0.5
June 1987
June 1988
June 1989
June 1990
June 1991
1987-1991 RMS Error (buoy minus satellite) - DAY & NIGHT
RMS = 0.82oC
RMS Error (degrees C)
3
2
1
0
June 1987
June 1988
June 1989
June 1990
June 1991

Figure 3

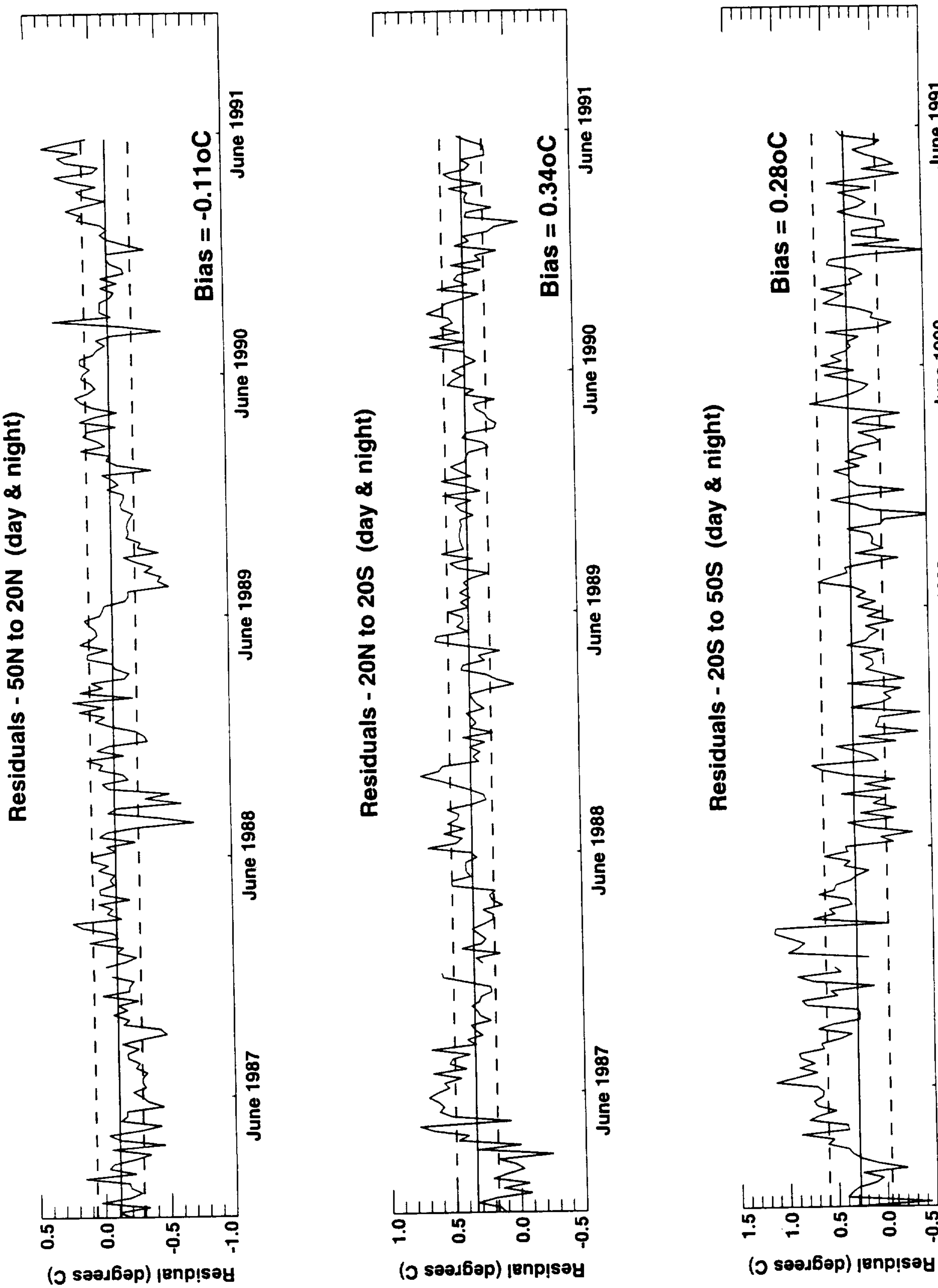

Residuals - 50N to 20N (day & night)
Bias = -0.11oC
Residual (degrees C)
0.5
0.0
-0.5
-1.0
June 1987
June 1988
June 1989
June 1990
June 1991
Residuals - 20N to 20S (day & night)
Bias = 0.34oC
Residual (degrees C)
1.0
0.5
0.0
-0.5
June 1987
June 1988
June 1989
June 1990
June 1991
Residuals - 20S to 50S (day & night)
Bias = 0.28oC
Residual (degrees C)
1.5
1.0
0.5
0.0
-0.5
June 1987
June 1988
June 1989
June 1990
June 1991

Figure 4

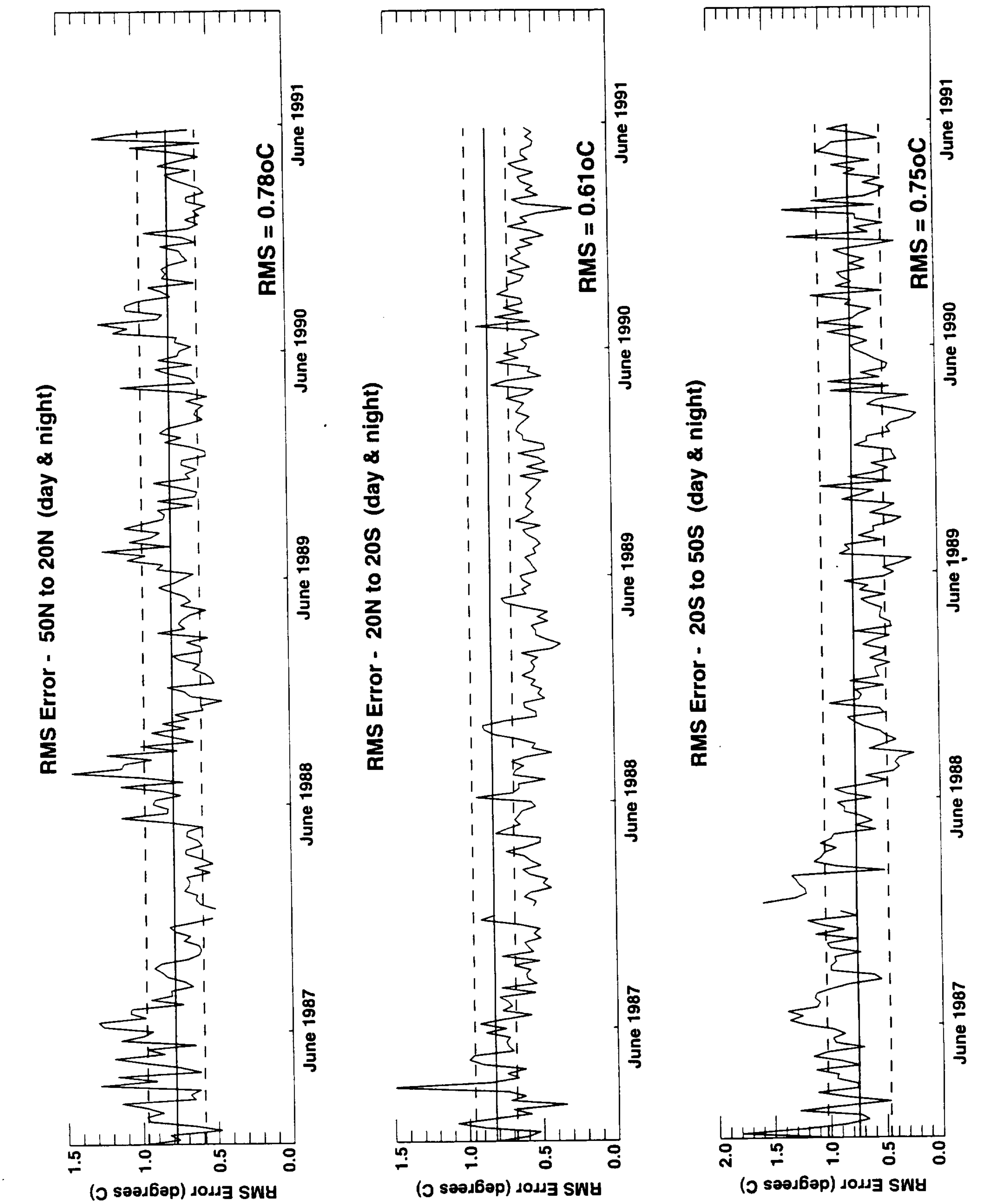

RMS Error - 50N to 20N (day & night)
RMS = 0.78oC
RMS Error (degrees C)
1.5
1.0
0.5
0.0
June 1987
June 1988
June 1989
June 1990
June 1991
RMS Error - 20N to 20S (day & night)
RMS = 0.61oC
RMS Error (degrees C)
1.5
1.0
0.5
0.0
June 1987
June 1988
June 1989
June 1990
June 1991
RMS Error - 20S to 50S (day & night)
RMS = 0.75oC
RMS Error (degrees C)
2.0
1.5
1.0
0.5
0.0
June 1987
June 1988
June 1989
June 1990
June 1991

Figure 5

This table shows a summary of the statistics for 1987 satellite/buoy matchups.

REGION	Day/Night	RMSD	BIAS	Y-intercept	# observations
Global	day&night	0.96	0.05	0.48	9616
	day	0.94	0.01	0.37	4234
	night	0.97	0.09	0.55	5382
Eastern Trop. Pacific	day&night	0.68	0.39	2.20	1953
	day	0.56	0.26	1.12	783
	night	0.74	0.49	1.37	1170
East Coast NA & G.O.M	day&night	0.89	-0.24	0.51	2002
	day	0.75	-0.20	-0.12	819
	night	0.97	-0.26	0.71	1183
North Atlantic	day&night	1.13	0.15	-0.15	220
	day	1.22	0.10	0.86	129
	night	0.99	0.22	-0.02	91
S. Indian & S. Atlantic	day&night	1.24	0.61	0.22	1241
	day	1.17	0.49	0.24	648
	night	1.31	0.74	0.21	593
West Coast NA & Eastern Pacific	day&night	0.76	-0.04	0.26	2376
	day	0.71	-0.07	0.10	997
	night	0.79	-0.01	0.24	1379
Indian Ocean	day&night	1.29	-0.25	11.79	215
	day	1.42	-0.62	14.0	104
	night	1.15	0.10	10.48	111

Table 2

This table shows a summary of the statistics for 1988 satellite/buoy matchups.

REGION	Day/Night	RMSD	BIAS	Y-intercept	# observations
Global	day&night	0.80	0.1	0.36	8834
	day	0.76	0.1	0.27	3930
	night	0.82	0.1	0.43	4904
Eastern Trop. Pacific	day&night	0.64	0.35	0.68	2348
	day	0.57	0.26	0.55	963
	night	0.68	0.42	0.45	1385
East Coast NA & G.O.M	day&night	0.82	-0.21	0.40	2472
	day	0.70	-0.12	-0.09	1028
	night	0.89	-0.27	0.54	1444
North Atlantic	day&night	1.15	0.41	-1.49	181
	day	1.24	0.37	1.90	119
	night	0.96	0.48	-1.32	62
S. Indian & S. Atlantic	day&night	1.08	0.35	0.47	733
	day	0.93	0.22	-0.26	414
	night	1.23	0.51	0.33	359
West Coast NA & Eastern Pacific	day&night	0.78	-0.04	0.58	2401
	day	0.83	-0.03	-0.13	1034
	night	0.74	-0.05	0.47	1367

Table 3

This table shows a summary of the statistics for 1989 satellite/buoy matchups.

REGION	Day/Night	RMSD	BIAS	Y-intercept	# observations
Global	day&night	0.75	0.02	0.31	8894
	day	0.73	-0.05	0.31	4393
	night	0.77	0.08	0.28	4501
Eastern Trop. Pacific	day&night	0.56	0.33	0.26	1814
	day	0.49	0.25	1.16	653
	night	0.59	0.38	0.22	1170
East Coast NA & G.O.M	day&night	0.82	-0.17	0.39	3023
	day	0.74	-0.15	-0.07	1196
	night	0.86	-0.18	0.50	1827
North Atlantic	day&night	1.59	0.32	0.43	193
	day	1.79	0.43	0.61	116
	night	1.21	0.15	-0.06	77
S. Indian & S. Atlantic	day&night	0.69	0.10	-0.20	879
	day	0.67	0.07	0.35	499
	night	0.71	0.14	-0.25	380
West Coast NA & Eastern Pacific	day&night	0.71	-0.11	0.51	2332
	day	0.71	-0.18	-0.11	1732
	night	0.72	0.10	0.19	600
Indian Ocean	day&night	0.70	0.48	3..48	37
	day	0.67	0.54	-2.24	15
	night	0.72	0.44	3.35	22

Table 4

This table shows a summary of the statistics for 1990 satellite/buoy matchups.

REGION	Day/Night	RMSD	BIAS	Y-intercept	# observations
Global	day&night	0.78	0.05	0.32	10875
	day	0.72	-0.04	0.33	4162
	night	0.82	0.10	0.29	6713
Eastern Trop. Pacific	day&night	0.63	0.36	-0.22	1764
	day	0.51	0.25	1.92	380
	night	0.66	0.39	-0.15	1384
East Coast NA & G.O.M	day&night	0.82	-0.18	0.52	3651
	day	0.71	-0.17	-0.10	1351
	night	0.88	-0.18	0.66	2300
North Atlantic	day&night	0.92	0.14	0.21	590
	day	0.75	-0.05	-0.05	245
	night	1.02	0.28	0.16	345
S. Indian & S. Atlantic	day&night	0.74	0.26	-0.12	787
	day	0.73	0.25	0.24	441
	night	0.75	0.27	-0.22	346
West Coast NA & Eastern Pacific	day&night	0.76	0.0	0.54	3080
	day	0.74	-0.14	-0.20	1406
	night	0.77	0.11	0.41	1674
Indian Ocean	day&night	1.1	0.95	-1.88	43
	day	1.19	1.02	11.32	18
	night	1.04	0.91	0.57	25

Table 5